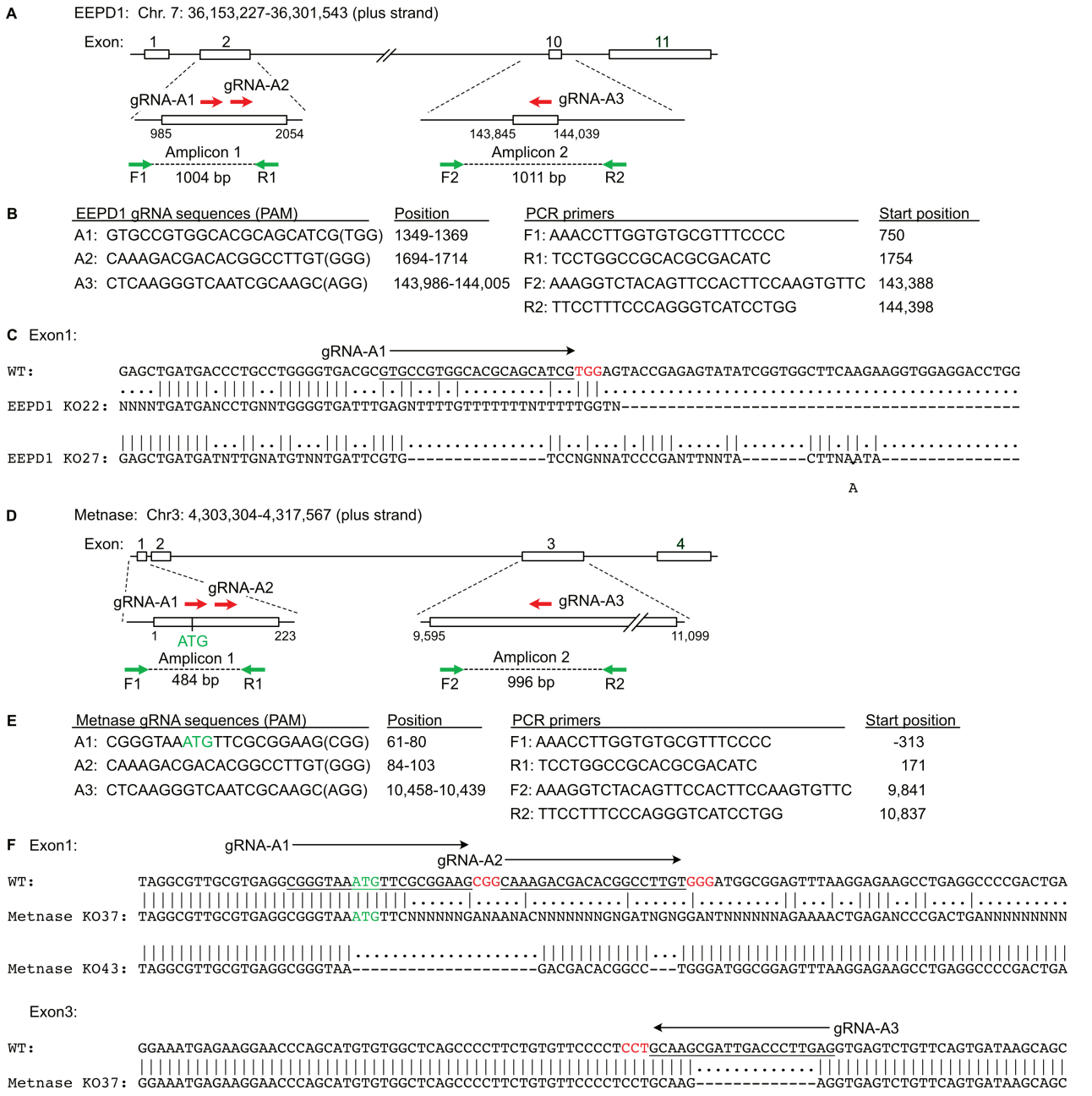

Figure S1. CRISPR KO strategies and sequence analysis of EEPD1 and Metnase KO loci. (A) Map of EEPD1 exons, locations of CRISPR gRNA targets, and PCR amplicons used for DNA sequence analysis. (B) Sequences and positions of EEPD1 gRNAs and PCR primers; position 1 is the first nt of exon 1. (C) Sequences from EEPD1 exon 1 region for WT (parental HeLa) and EEPD1 KO mutants #22 and #27. Two gRNA targets are underlined in the WT sequence and graphically above; the PAM site is shown in red font. (D-F) Metnase maps, gRNA/PCR sequences, and exon 1 and exon 3 sequences from WT and KO loci as described in panels A-C. The Metnase ATG start codon is shown in green font. T7E1 assays showed indels in exon 1 and/or 3 (not shown) in Metnase KO #25 and #37, consistent with Western blot results (Fig. 1), but sequence analysis of these loci was inconclusive.

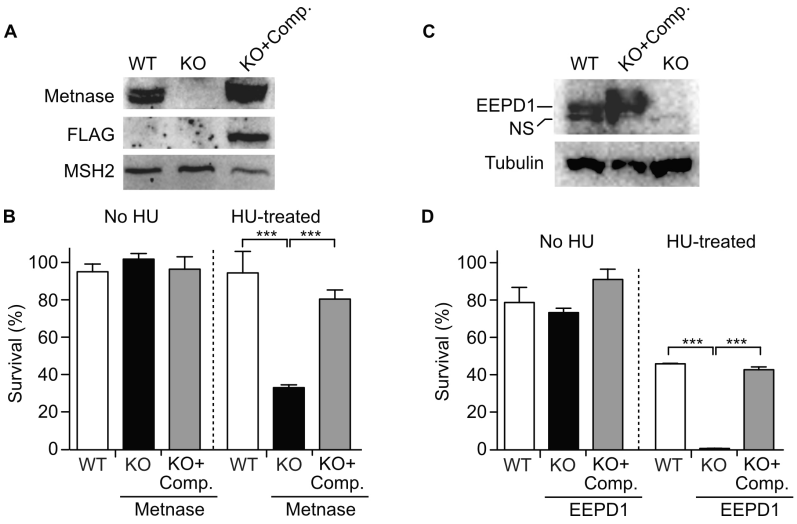

Figure S2. Complementation of Metnase and EEPD1 KO cells. (A) Western blot of parent HeLa (WT), Metnase KO, and KO cells complemented with FLAG-tagged WT Metnase, probed with antibodies to Metnase or FLAG, or MSH2 as loading control. (B) Complementation of Metnase KO with WT Metnase restores HU sensitivity to level similar to parent HeLa cells. (C,D) EEPD1 KO cells were complemented with FLAG- and Myc-tagged WT EEPD1. Western blot and HU sensitivity are shown as described in panels A and B, with tubulin as loading control (NS, non-specific signal). The dual epitope tags noticeably retard gel migration of complementing EEPD1.

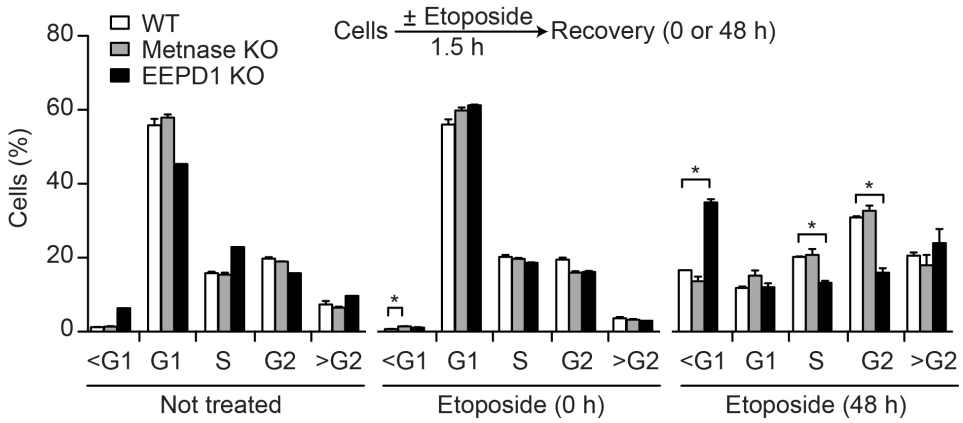

Figure S3. Cell cycle distributions of WT, Metnase KO and EEPD1 KO cells incubated with or without 20 μM etoposide for 1.5 h, and DNA content was analyzed by flow cytometry after 0 or 48 h. Values are averages (±SD) for 2 determinations; statistics calculated by t tests.

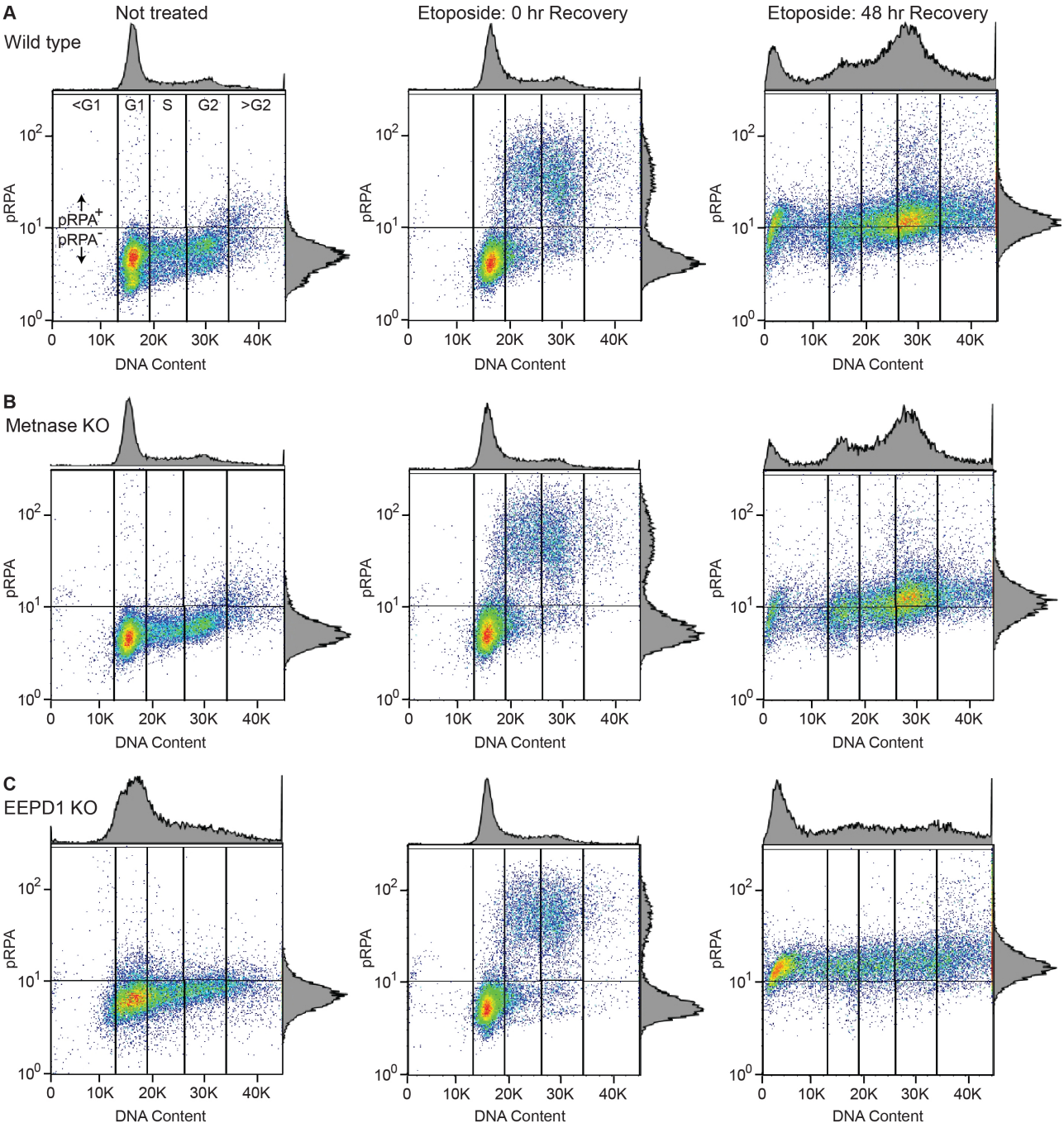

Figure S4. Representative flow cytometry scatter plots of pRPA signals and DNA content. Vertical lines indicate cell cycle gates of sub-G1, G1, S, G2, and hyper-G2 DNA content, and the horizontal line indicates populations that are pRPA positive (above) or negative (below). Histograms of DNA content and pRPA signals and shown at the top and right, respectively. **(A)** WT HeLa cells. **(B)** Metnase KO cells. **(C)** EEPD1 KO cells.

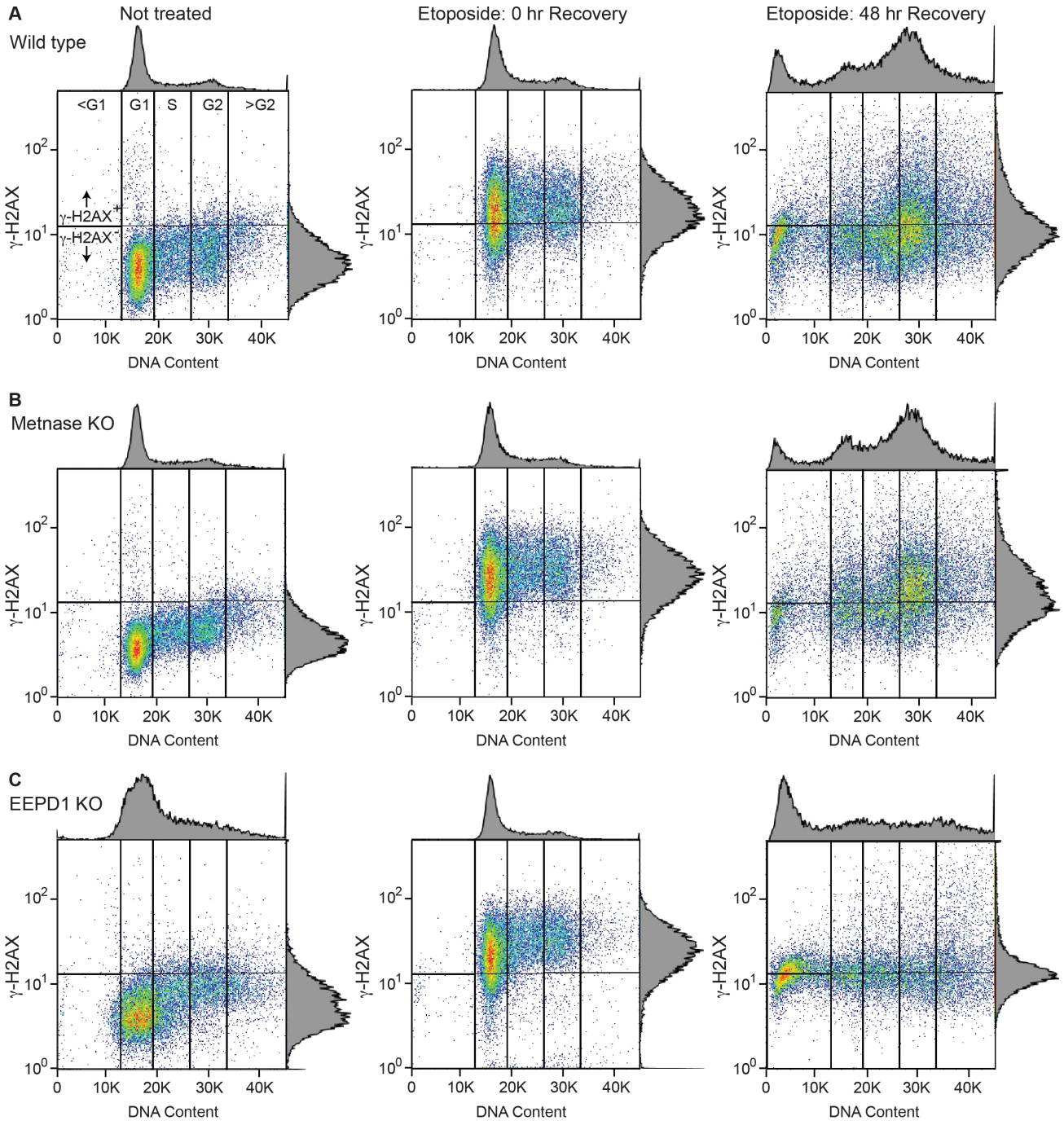

Figure S5. Representative flow cytometry scatter plots of γ-H2AX signals and DNA content, as described in Figure S2.

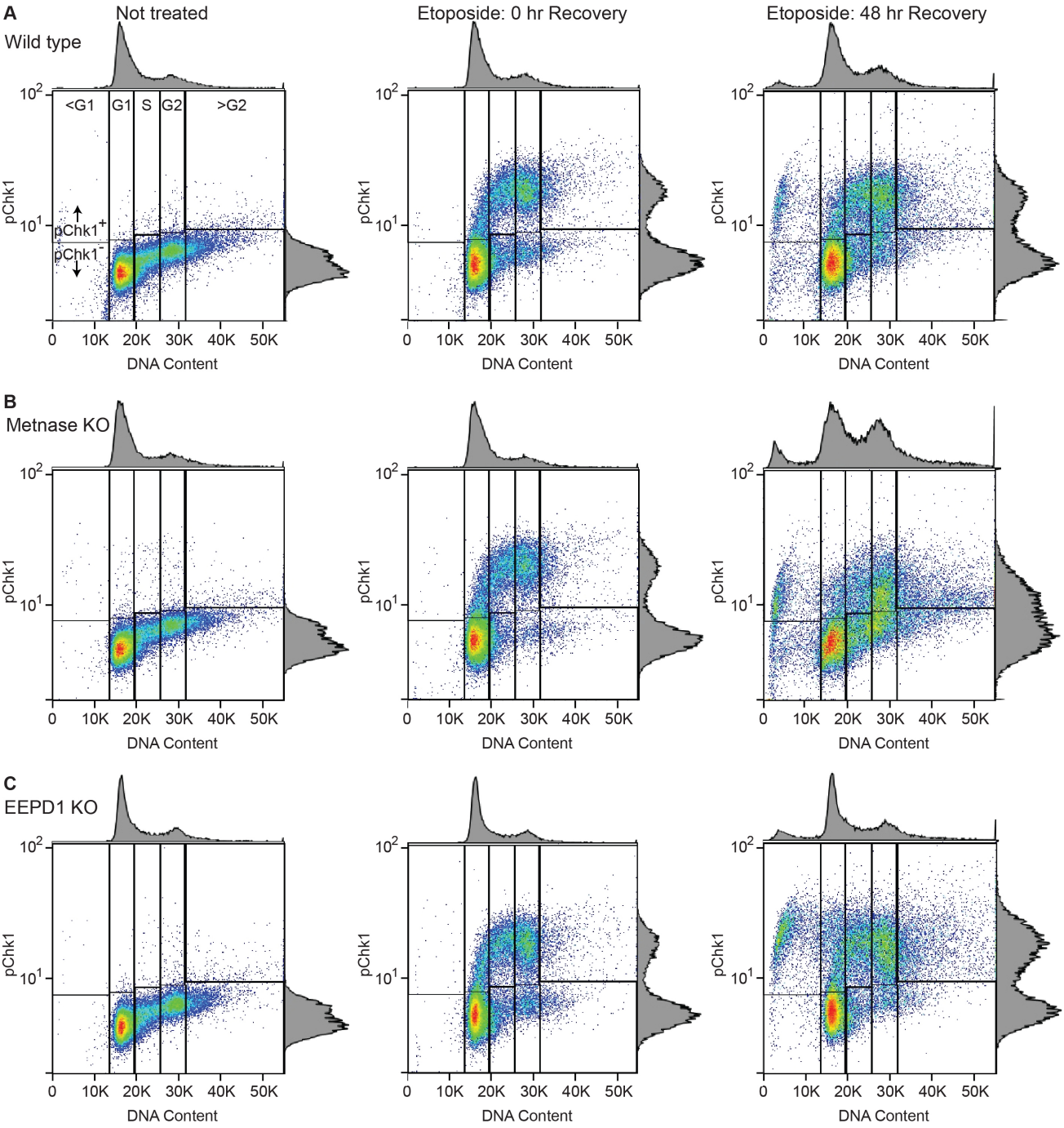

Figure S6. Representative flow cytometry scatter plots of pChk1 signals and DNA content, as described in Figure S2.

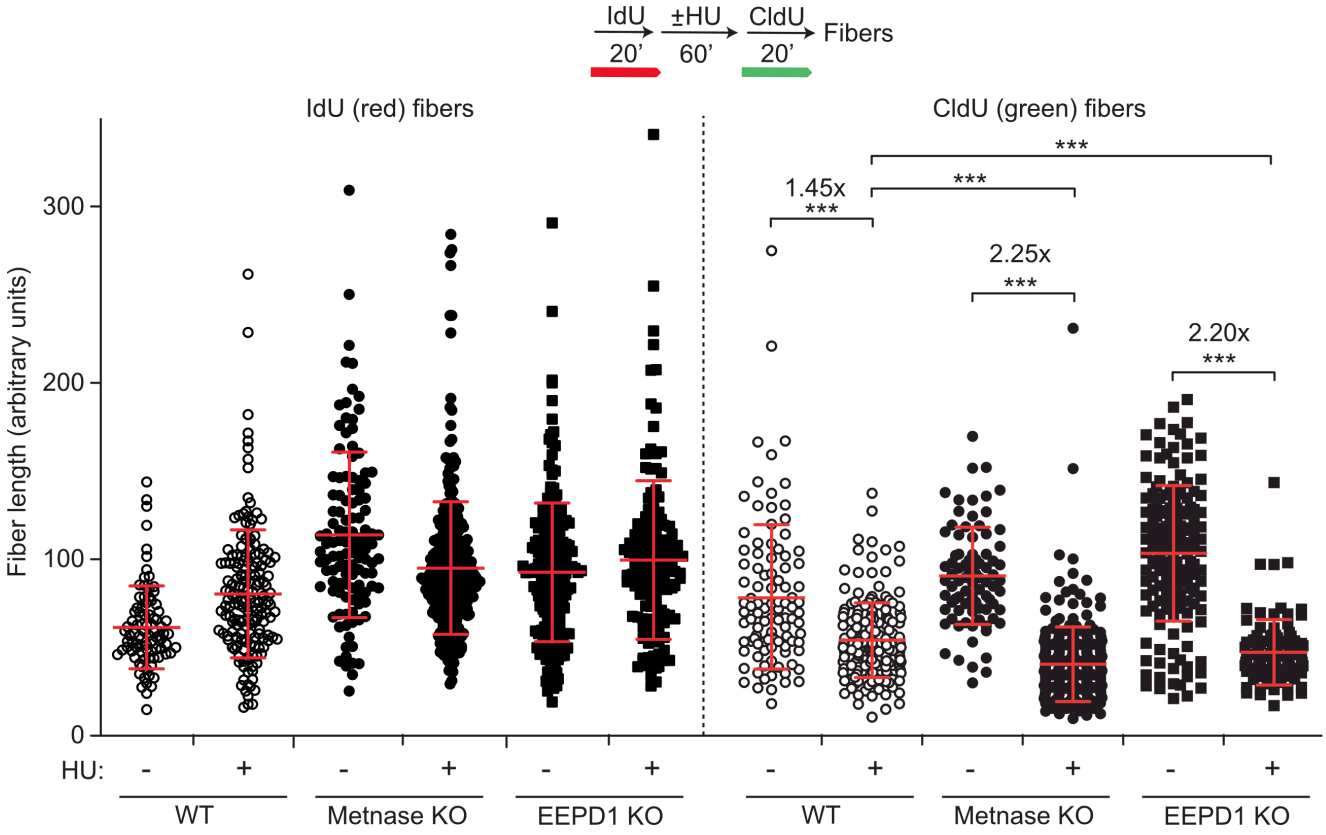

Figure S7. Delayed fork restart in Metnase KO and EEPD1 KO cells. Individual IdU (red) and CldU (green) fiber lengths for untreated or HU-treated cells are plotted. IdU fiber lengths are pooled because IdU was incorporated prior to HU treatment. Mean fiber lengths (±SD) are indicated by red lines and error bars; statistics calculated by t tests.

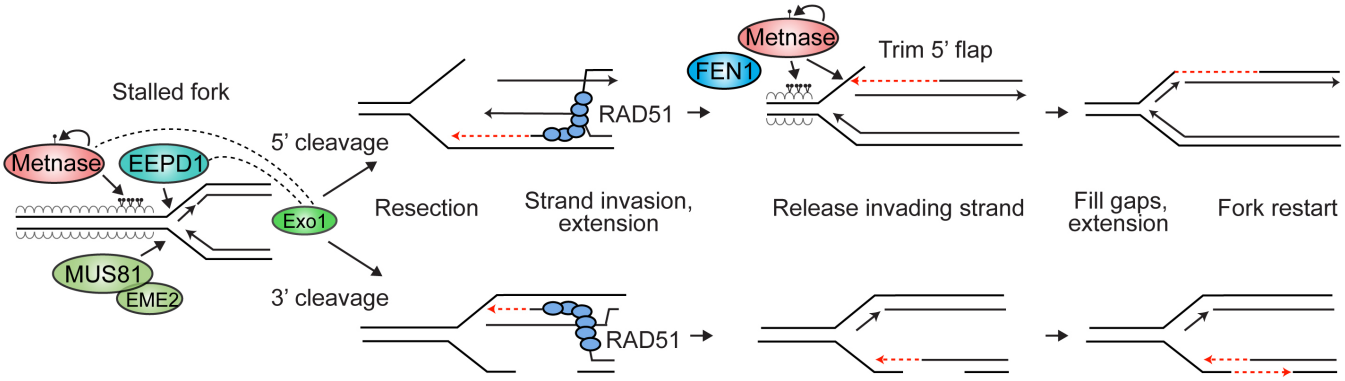

Figure S8. Model for EEPD1 and Metnase roles in replication fork restart. At stalled forks Metnase di-methylation of H3K36 (lollipop symbols) recruits DDR factors, and automethylation promotes its cleavage of branched structures. EEPD1 cleaves the stalled fork, and both Metnase and EEPD1 promote recruitment of Exo1 to resect ends and drive repair toward accurate, HR-mediated fork restart. RPA (not shown) and then RAD51 is loaded onto ssDNA, which invades the sister chromatid, is extended (dashed lines), and is then released to reestablish the fork. Metnase trims the 5' flap (redundant with FEN1) or other branched structures like regressed forks (chicken feet; not shown). Metnase may methylate H3K36 and itself at early and late stages. Cleavage by the 3' nuclease MUS81/EME2 initiates fork restart by an alternative pathway, below.